Quaternion-based attitude sliding mode control with disturbance rejection observer for a quadrotor

J. Ayala-Olivares[*], R. Enriquez-Caldera[†], and J.F. Guerrero-Castellanos[‡]
Intituto Nacional de Astrofísica Óptica y Electrónica, Benemérita Universidad Autónoma de Puebla

ABSTRACT

This work presents a Slide Mode Control (SMC) for the attitude of a quadrotor under unknown disturbances and whose main characteristic is the use of the quaternion mathematics for modeling the system. An extended state observer (ESO) is designed to estimate unknown disturbances and uncertainties. Tests are carried under a previously defined smooth trajectory and the reference quaternion is calculated, and the controller is able to follow the reference to keep the desire orientation. Numerical simulation is shown in order to demonstrate the effectiveness of the proposed control law.

1 INTRODUCTION

1.1 Motivation and Background

A quadrotor is a multi-engine helicopter powered by four engines. These vehicles are easy to build and maintain, and allow very good maneuverability in three-dimensional spaces. In their early days, these vehicles were very poor in terms of computational power, payload capacity and maneuverability. However, given the advances in electronics, which on the hardware side have allowed the miniaturization of its components, and on the software side has allowed the flexibility of the tasks, it has been achieved that today the quadrotors are much smaller, lighter and with such computational power that has resulted in vehicles to perform some tasks autonomously [1].

Two subsystems can be considered when dealing with mathematical models of quadrotors: rotational and translation dynamics [2]. These subsystems provide a cascade structure where translational motion is based on rotational dynamics [3]. Therefore, attitude control is the main part to fulfill trajectory-tracking in the space. This is not a simple task when considering both structural (parametric) and external disturbances. For these reasons, it is necessary to come back to the low-level control problem, i.e., the attitude control problem, and therefore to take into account explicitly in the control design model uncertainties and external disturbances.

In the literature, there are two predominant mathematical models for the quadrotor representation. The most used is obtained by using an Euler's angles representation, allowing a more intuitive understanding of the behavior of the vehicle (see [4, 5]); the second model is based in quaternions offer a compact representation for vehicle's orientation in a 3-D space that is convenient, computationally efficient, and accurate [6, 7, 8].

Both models have disadvantages, for example: the model with Newton-Euler equations is a system of 12 nonlinear differential equations and, in general, to solve them requires a high computational cost and the consequent loss of information in the process due to the numerical methods applied; on the other hand, the model with quaternions is difficult to interpret due to the abstract nature of its theory [9].

Several linear control approaches, such as PID ([10]), Linear Quadratic Regulator (LQR) ([11]) and Linear Quadratic Gaussian (LQG) ([12]), have been proposed in the literature and applied for attitude stabilization and/or altitude tracking of quadrotors. However, these methods can impose limitations on application of quadrotors for extended flight complex flight trajectories where the system is no longer linear. In addition, the performances on tracking trajectories of these control laws are not satisfactory enough [13, 14].

To overcome the linear controllers limitations, there are nonlinear control alternatives, such as Backstepping [15, 16, 17], Feedback linearization [18, 19], Model predictive control [20, 21, 22], among others. These control techniques have shown good performance against sinusoidal wind disturbance but increasing the cost of computational resources [23].

The Sliding Mode Control has been applied extensively to control quadrotors. The primary advantages of SMC are: 1. Fast response and good transient performance. 2. Its robustness against a large class of perturbations or model uncertainties. 3. The possibility of stabilizing some complex nonlinear systems which are difficult to stabilize by continuous state feedback laws [24]. The SMC is a high frequency switching control that causes chattering, an undesired phenomenon which leads towards loss of energy, unmodeled dynamics and even actuator destruction [25].

Furthermore, to enhance performance robustness, an Extended State Observer can be implemented. An ESO can estimate both, unknown states of system and the "total disturbances" that lump the adverse effects on the output using limited model information [26].

[*]Email address: jrayala@inaoe.mx
[†]Email address: rogerio@inaoe.mx
[‡]Email address: fermi.guerrero@correo.buap.mx

1.2 Contributions

The development of a SMC for attitude tracking of a quadrotor with a ESO applied to the quaternion-based model, adding disturbances to the inertial matrix and input control torques.

This paper is organized as follows. The basic concepts of quaternion theory and dynamic model of a quadrotor are presented in Sect.2. In Sect.3, the position control is described, following by the SMC concepts and the attitude controller is designed, later, an ESO is proposed and designed. The simulation results of the proposed controller strategies are presented in Sect.4. Finally, conclusions are included in Sect.5.

2 QUATERNION BACKGROUND AND QUADROTOR MODELING

A quaternion background is shown next, and the quadrotor model based on quaternions as well.

2.1 Quaternions

A quaternion can be thought as a composite of a scalar $q_0 \in \mathbb{R}$ and an ordinary vector $\mathbf{q}_v = (q_1\ q_2\ q_3)^T \in \mathbb{R}^3$, that is, $\mathbf{q} = (q_0\ \mathbf{q}_v^T)^T$ or as a complex number with three different imaginary parts, *i.e.*, a hypercomplex number [27]. It is represented as follows

$$\mathbf{q} := \begin{pmatrix} q_0 \\ \mathbf{q}_v \end{pmatrix} = q_0 + \mathbf{i}q_1 + \mathbf{j}q_2 + \mathbf{k}q_3 \in \mathbb{H} \tag{1}$$

with $\{1, \mathbf{i}, \mathbf{j}, \mathbf{k}\}$ being a canonical basis of the hypercomplex space $\mathbb{H}$ [7]. The norm of a quaternion is

$$||\mathbf{q}|| = \sqrt{q_0^2 + q_1^2 + q_4^2 + q_3^2} \tag{2}$$

A unit quaternion, with a norm equal to 1, can be used to represent a rotation by an angle β about the axis defined by the unit vector $\mathbf{e} = (e_1\ e_2\ e_3)^T$, that is

$$\mathbf{q} := e^{\frac{1}{2}\beta\mathbf{e}} = \cos\frac{\beta}{2} + \mathbf{e}\sin\frac{\beta}{2} \tag{3}$$

This expression, known as the Euler-Rodrigues formula is the exponential mapping of the axis-angle representation of a rotation. Since the n-dimensional unit sphere embedded in $\mathbb{R}^{n+1}$ is denoted as $\mathbb{S}^n = \{\mathbf{x} \in \mathbb{R}^{n+1} : \mathbf{x}^T\mathbf{x} = 1\}$ then $\mathbf{q} \in \mathbb{S}^3$. Furthermore, $\mathbf{q}$ represents an element of $SO(3)$ through the map $\mathbf{R} : \mathbb{S}^3 \to SO(3)$ defined as:

$$\mathbf{R}(\mathbf{q}) := I_3 + 2q_0[\mathbf{q}_v^\times] + 2[\mathbf{q}_v^\times]^2 \tag{4}$$

$\mathbf{R} \in SO(3) = \{\mathbf{R} \in \mathbb{R}^{3\times3} : \mathbf{R}^T\mathbf{R} = I_3, \det(\mathbf{R}) = 1\}$ is the matrix that rotates the coordinates of a point from frame $\mathbf{E}^b$ to frame $\mathbf{E}^f$ with I_3 as the 3×3 identity matrix. $[\mathbf{r}^\times]$ is the skew-symmetric matrix associated to vector $\mathbf{r}$.

The sum and subtraction of quaternions is performed by separate addition of their four parts. A vector can be converted to quaternion by setting the scalar part to zero and replacing the vector part of the quaternion by the corresponding values of the vector. The quaternion product is defined as

$$\mathbf{q} \otimes \mathbf{r} = (q_0 r_0 - \mathbf{q}_v \cdot \mathbf{r}_v) + (q_0\mathbf{r}_v + r_0\mathbf{q}_v + \mathbf{q}_v \times \mathbf{r}_v) \tag{5}$$

The conjugate of a unit quaternion is defined as $\mathbf{q}^* = q_0 - \mathbf{q}_v$.

$$\mathbf{q}^* = q_0 - \mathbf{q}_v \tag{6}$$

A quaternion can be used as rotation operator for a vector between two different frames. Considering $\mathbf{p}_v$ as a 3D vector in a given reference frame $\mathbf{E}^f$ and $\mathbf{p}'_v$ as the same vector in a new different frame, for instance, $\mathbf{E}^b$. Then, the quaternion $\mathbf{p} = (0\ \mathbf{p}_v^T)^T$ can be transform in $\mathbf{p}'$, and vice-versa through

$$\mathbf{p}' = \mathbf{q}^* \otimes \mathbf{p} \otimes \mathbf{q}, \quad \mathbf{p} = \mathbf{q} \otimes \mathbf{p} \otimes \mathbf{q}^* \tag{7}$$

The properties of the logarithm in the unit quaternion are useful to obtain the equivalent axis-angle notation. For unitary quaternions the logarithmic mapping is given by

$$\ln(\mathbf{q}) = \begin{cases} \frac{\mathbf{q}_v}{\|\mathbf{q}_v\|}\arccos\ q_0, & \|\mathbf{q}_v\| \neq 0 \\ (0\ 0\ 0)^T & \|\mathbf{q}_v\| = 0 \end{cases} \tag{8}$$

With this mapping you can change any unitary quaternion to its axis-angle representation as follows [7]

$$\begin{aligned} \boldsymbol{\beta}_v &= \mathbf{e}\beta = 2\ln(\mathbf{q}) \in \mathbb{R}^3 \\ \dot{\boldsymbol{\beta}}_v &= \boldsymbol{\omega}_v \in \mathbb{R}^3 \end{aligned} \tag{9}$$

where $\boldsymbol{\beta}_v$ is the vector that represents the axis-angle notation, $\mathbf{e} = \frac{\mathbf{q}_v}{\|\mathbf{q}_v\|}$ describes the unit axis about which the rotation is applied, $\|\beta\|$ represents the magnitude of the rotation. $\boldsymbol{\omega}_v$ is the angular velocity vector of the body coordinate frame $\mathbf{E}^b$ relative to the inertial coordinate frame $\mathbf{E}^f$ expressed in $\mathbf{E}^b$. The attitude error is used to quantify the mismatch between two attitudes. If $\mathbf{q}$ defines the current attitude quaternion and $\mathbf{q}_d$ the desired quaternion, *i.e.*, the desired orientation, then the quaternion that represents the attitude error between the current orientation and the desired one is given by [28]:

$$\tilde{\mathbf{q}} = \mathbf{q}_d^* \otimes \mathbf{q} = \begin{pmatrix} \tilde{q}_0 & \tilde{\mathbf{q}}_v^T \end{pmatrix}^T \tag{10}$$

When the current quaternion $\mathbf{q}$ reaches the desired one $\mathbf{q}_d$, the quaternion error becomes $\tilde{\mathbf{q}} = \begin{pmatrix} \pm 1 & 0^T \end{pmatrix}^T$, *i.e.*, there exist two equilibria which have to be considered in the stability analysis [29].

2.2 Quadrotor Dynamics

A diagram of the quadrotor studied in this paper is shown in Fig. 1, where the inertial frame and the body frame are represented by $\mathbf{E}^f$ and $\mathbf{E}^b$, respectively. Let define the position vector $\mathbf{p} = \begin{bmatrix} x & y & z \end{bmatrix}^T$. Then, the related quaternion is given by $\xi = [0\ \mathbf{p}^T]^T$

According to [7, 30, 31], the equations of motion of a quadrotor using quaternions are

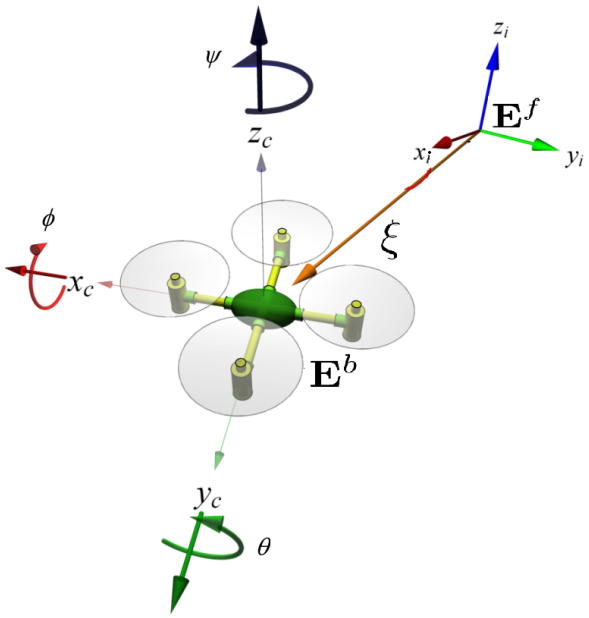

Figure 1: Quadrotor diagram.

$$\dot{X} = \frac{d}{dt}\begin{bmatrix} \xi \\ \dot{\xi} \\ \mathbf{q} \\ \omega \end{bmatrix} = \begin{bmatrix} \dot{\xi} \\ \mathbf{q} \otimes \frac{F_{th}}{m} \otimes \mathbf{q}^* + \bar{g} \\ \frac{1}{2}\mathbf{q} \otimes \boldsymbol{\omega} \\ J^{-1}(\tau - \boldsymbol{\omega}_v \times J\boldsymbol{\omega}_v) \end{bmatrix} \tag{11}$$

where $\mathbf{q}$ represents the vehicle attitude, using a unit quaternion, with respect to the inertial frame, $\boldsymbol{\omega} = [0\ \boldsymbol{\omega}_v]^T$ and $F_{\text{th}} = \begin{bmatrix} 0 & 0 & 0 & \sum_{i=1}^{4} f_i \end{bmatrix}^T$ describes the total thrust force applied to the body in the inertial frame, and the angular velocity. J represents the inertia matrix with respect to the body-fixed frame, and the total torque τ is given by

$$\tau = \begin{bmatrix} l\,(f_1 + f_4 - f_2 - f_3) \\ l\,(f_1 + f_4 - f_2 - f_3) \\ \sum_{i=1}^{4} (-1)^{i+1}\tau_i \end{bmatrix}, \tag{12}$$

where l represents the distance between any motor and the center of mass of the vehicle, f_i represents the force generated in the rotor i, with $i \in \{1, 2, 3, 4\}$. $\bar{g} = [0\ 0\ 0\ g]^T$ is the gravity vector.

Applying the logarithmic mapping, the system model is as follows

$$\dot{X} = \frac{d}{d\,t}\begin{bmatrix} \xi \\ \dot{\xi} \\ \boldsymbol{\beta}_v \\ \dot{\boldsymbol{\beta}}_v \end{bmatrix} = \begin{bmatrix} \dot{\xi} \\ \mathbf{q} \otimes \frac{F_{\text{th}}}{m} \otimes \mathbf{q}^* + \bar{g} \\ \dot{\boldsymbol{\beta}}_v \\ J^{-1}\left(\tau - \dot{\boldsymbol{\beta}}_v \times J\dot{\boldsymbol{\beta}}_v\right) \end{bmatrix} \tag{13}$$

3 QUADROTOR CONTROL

In this section, the control strategy is described, as is shown in the Fig. 2, position control allows the vehicle to follow a defined trajectory, then the attitude control is designed to achieve the necessary orientation given by the position control.

3.1 Position Control

The position dynamics subsystem of the quadrotor can be written as

$$\dot{\xi} = \frac{d}{dt}\begin{bmatrix} \xi \\ \dot{\xi} \end{bmatrix} = \begin{bmatrix} \dot{\xi} \\ m^{-1}F_{\text{th}}^I \end{bmatrix} \tag{14}$$

where $F_{\text{th}}^I = \mathbf{q} \otimes F_{\text{th}} \otimes \mathbf{q}^* + m\bar{g}$ is a force that can be designed such that the vehicle reach a desired position. Since Equation 14 is a linear system, the control law F_{th}^I is proposed as

$$F_{\text{th}}^I = \ddot{\xi}_d + k_1\tilde{\xi} + k_2\dot{\tilde{\xi}} \tag{15}$$

where ξ_d is the desired position, $\tilde{\xi} = \xi_d - \xi$ is the position error, with k_1 and k_2 are the control gains. The error dynamics is given by

$$\frac{d}{dt}\begin{bmatrix} \tilde{\xi} \\ \dot{\tilde{\xi}} \end{bmatrix} = \begin{bmatrix} \dot{\tilde{\xi}} \\ \ddot{\xi}_d - (\ddot{\xi}_d - k_1\tilde{\xi} + k_2\dot{\tilde{\xi}}) \end{bmatrix} \tag{16}$$

rewriting equation (16)

$$\frac{d}{dt}\begin{bmatrix} \tilde{\xi} \\ \dot{\tilde{\xi}} \end{bmatrix} = \underbrace{\begin{bmatrix} 0 & 1 \\ k_1 & k_2 \end{bmatrix}}_{A}\begin{bmatrix} \tilde{\xi} \\ \dot{\tilde{\xi}} \end{bmatrix} \tag{17}$$

if $k_1, k_2 > 0$ then A is Hurwitz and the trajectories of the error dynamics converge asymptotically to the origin of the vector space error, that is, $\tilde{\xi}, \dot{\tilde{\xi}} \to 0$, when $t \to \infty$.

3.2 Basic concepts of Slide mode control

The SMC is a type of Variable Structure Control (VSC). Its basic idea is to attract the system states towards a surface, called sliding surface, suitably chosen and design a stabilizing control law that keeps the system states on such a surface. For the choice of the sliding surface shape, the general form of equation (18) was proposed by Stoline and Li in [13]:

$$S(x) = \left(\lambda_x + \frac{d}{dt}\right)^{q-1} e(x) \tag{18}$$

where x denotes the variable control (state), $e(x)$ is the tracking error defined as $e(x) = x - xd$, λ_x is a positive constant that interprets the dynamics of the surface and q is the relative degree of the sliding mode controller.

Attractiveness is the condition under which the state trajectory will reach the sliding surface. There are two types of conditions of access to the sliding surface. In this paper, we will use the Lyapunov based approach. It consists of make

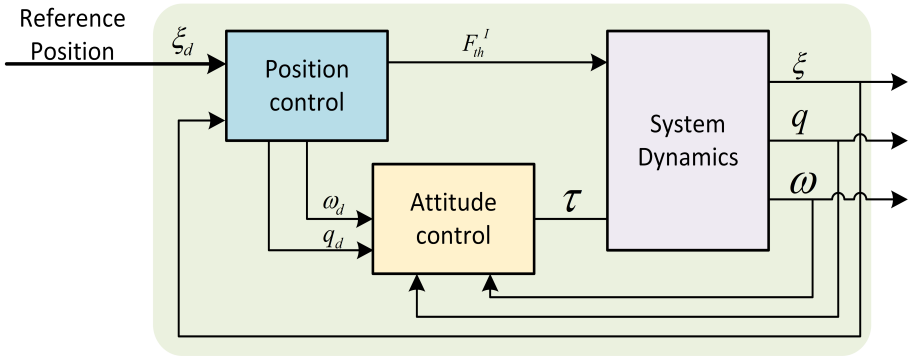

Figure 2: Control Block Diagram.

a positive scalar function, given by equation (19) and called Lyapunov candidate function, for the system state variables and then choose the control law that will decrease this function:

$$\dot{V}(x) < 0, \text{ with } V(x) > 0 \tag{19}$$

In this case, the Lyapunov function can be chosen as:

$$V(x) = \frac{1}{2}S(x)^2 \tag{20}$$

The derivative of this above function is negative when the following expression is checked:

$$S(x)\dot{S}(x) < 0 \tag{21}$$

The purpose is to force the system state trajectories to reach the sliding surface and stay on it despite the presence of uncertainty. The sliding control law contains two terms as follows:

$$u(t) = u_{eq}(t) + u_D(t) \tag{22}$$

where $u_{eq}(t)$ denotes the equivalent control, which is a way to determine the behavior of the system when an ideal sliding regime is established. it is calculated from the following invariance condition of the surface:

$$\begin{cases} S(x,t) = 0 \\ \dot{S}(x,t) = 0 \end{cases} \tag{23}$$

and $u_D(t)$ is a discontinuous function calculated by checking the condition of the attractiveness. It is useful to compensate the uncertainties of the model and often defined as follows:

$$u_D(t) = -K\text{sign}(S(t)) \tag{24}$$

where K is a positive control parameter and sign$(\cdot)$ is the sign operator.

3.3 Attitude Control design

For the attitude control, we use the rotational motion model given by equation (13), we take the error quaternion $\tilde{\mathbf{q}}$ from Equation 10 and applying the logarithm mapping to $\tilde{\mathbf{q}}$ we get

$$\begin{aligned} \tilde{\mathbf{q}} &= \mathbf{q}_d^* \otimes \mathbf{q} \\ \tilde{\boldsymbol{\beta}}_v &= 2\ln(\tilde{\mathbf{q}}) \end{aligned} \tag{25}$$

$\mathbf{q}_d$ is obtained from the shortest rotation between F_{th} and F_{th}^I vectors as unitary vectors. According to [7] $\mathbf{q}_d$ is defined as

$$\mathbf{q}_d = \exp\left(\ln\left(F_{\text{th}}^I \otimes F_{\text{th}}^*\right)/2\right) \otimes \exp\left(\mathbf{q}_{\psi_d}\right)/2 \tag{26}$$

where $\mathbf{q}_{\psi_d} = \begin{bmatrix} 0 & 0 & 0 & \psi_d \end{bmatrix}^T$ is the desired rotation around the z axis.

The sliding surface is chosen based on the tracking error, such as:

$$S = \dot{\tilde{\boldsymbol{\beta}}}_v + \lambda\tilde{\boldsymbol{\beta}}_v \tag{27}$$

Deriving S, we get

$$\dot{S} = \dot{\omega}_e + \lambda\omega_e \tag{28}$$

where $\omega_e = \omega - \omega_d$ is the rotation velocity error, and ω_d is the desired rotation velocity which is defined as

$$\omega_d = 2\frac{d}{dt}(\ln \mathbf{q}_d) \tag{29}$$

Substituting the model values on equation (28), we get

$$\begin{aligned} \dot{S} &= \dot{\omega} - \dot{\omega}_d + \lambda(w - w_d) \\ \dot{S} &= J^{-1}(\tau - \omega \times J\omega) - \dot{\omega}_d + \lambda(w - w_d) \end{aligned}$$

Finally, the control law is obtained using Equation 22:

$$\tau = J(-(-J^{-1}\omega \times J\omega - \dot{\omega}_d + \lambda(\omega - \omega_d)) + u_D)$$
$$u_D = -K\text{sign}(S)$$

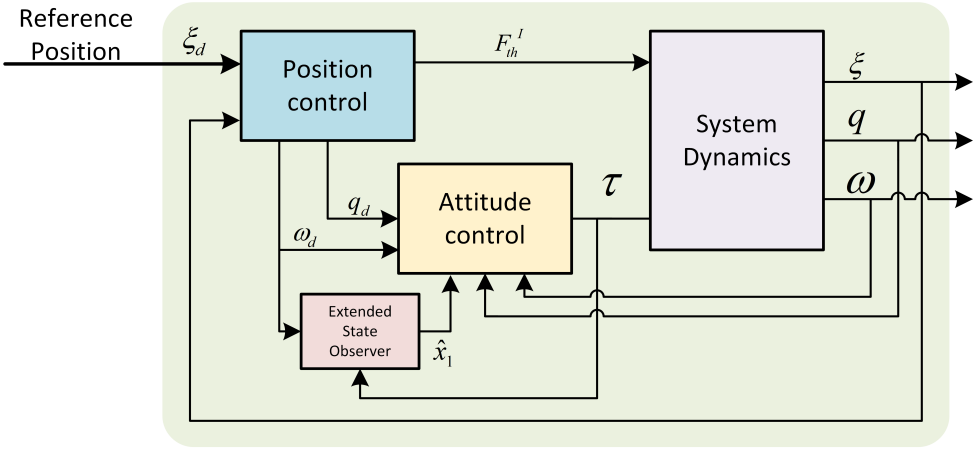

Figure 3: ESO attitude Control Block Diagram.

3.4 *ESO design*

The ESO of quadrotor UAV system should be designed to estimate the model uncertainties and external disturbances [32]. Fig. 3 shows the ESO implementation in the attitude control loop.

The attitude subsystem can be written as

$$\begin{bmatrix} \mathbf{q} \\ \omega \end{bmatrix} = \begin{bmatrix} \frac{1}{2}\mathbf{q} \otimes \omega \\ J^{-1}(\tau - \omega_v \times J\omega_v) \end{bmatrix} \tag{30}$$

In order to use the ESO for the estimation of uncertainties in the inertia matrix and unknown disturbances, ESO is defined as:

$$\begin{aligned} \dot{\hat{x}}_1 &= \hat{x}_2 + l_2(x_1 - \hat{x}_1) - J^{-1}\tau \\ \dot{\hat{x}}_2 &= l_1(x_1 - \hat{x}_1) \end{aligned} \tag{31}$$

where $\hat{x}_1$ is the estimation of the angular velocity ω, and $\hat{x}_2$ is the estimated value of an unknown disturbance d. l_1 and l_2 are the observer tuning parameters.

4 RESULTS

In this section, the proposed control strategy for the quadrotor attitude stabilization is implemented in order to verify his validity and efficiency. For the numerical simulation, the following parameters are using

$$m = 1.3\,\text{kg},\ J = \begin{bmatrix} 0.177 & 0 & 0 \\ 0 & 0.177 & 0 \\ 0 & 0 & 0.354 \end{bmatrix} \text{kg m}^2 \tag{32}$$

For the position controller, the control gains were empirically selected as: $k_1 = -24$ and $k_2 = -12$. In the same manner, the attitude control gains λ and K were selected as

$$\lambda = 10,\ K = 50 \tag{33}$$

4.1 *SMC sans ESO*

The dynamic model was coded using MATLAB, the chosen trajectory was a spiral as is shown in Fig. 4 with the following initial conditions: $\xi_d = [5\,5\,0]^T$m, $\xi = [0\,0\,0]^T$m and $[\phi\,\theta\,\psi]^T = [0\,0\,0]^T$rad. In addition, a uniform noise, $\pm 20\%$ of nominal value, is added to the inertial matrix and a sine wave $d = 0.1\sin(t)$ is applied as a disturbance in the control torques τ_1 and τ_2 signals @t=50s.

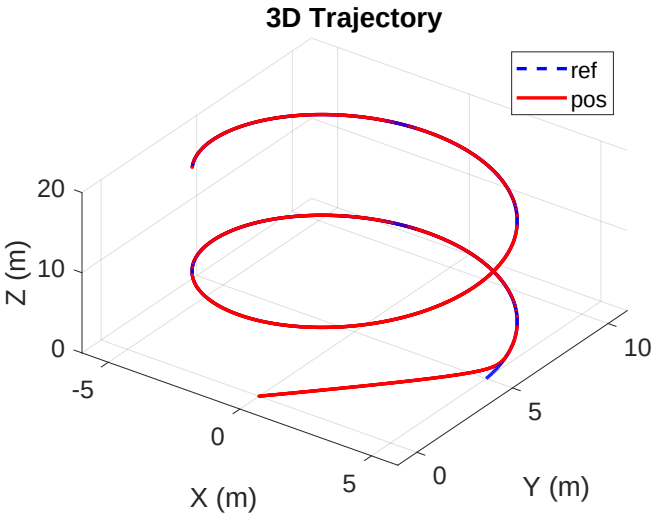

Figure 4: 3D spiral trajectory.

The position errors are shown in the Fig. 5

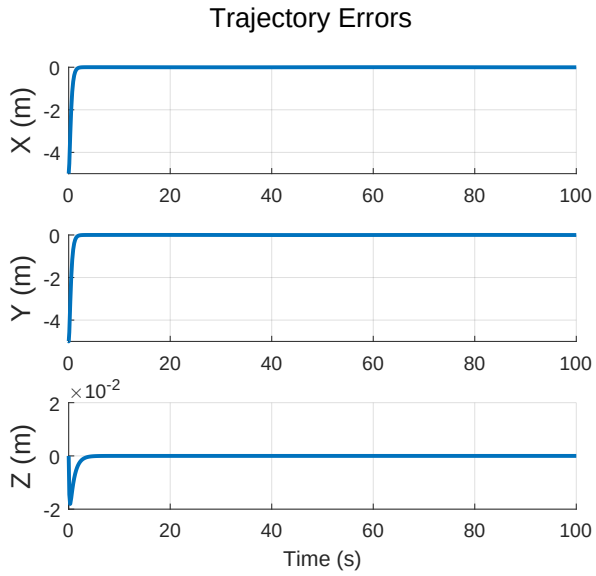

Figure 5: Errors in 3D trajectory.

The desired quaternion and the vehicle's attitude quaternion are shown in the Fig. 6.

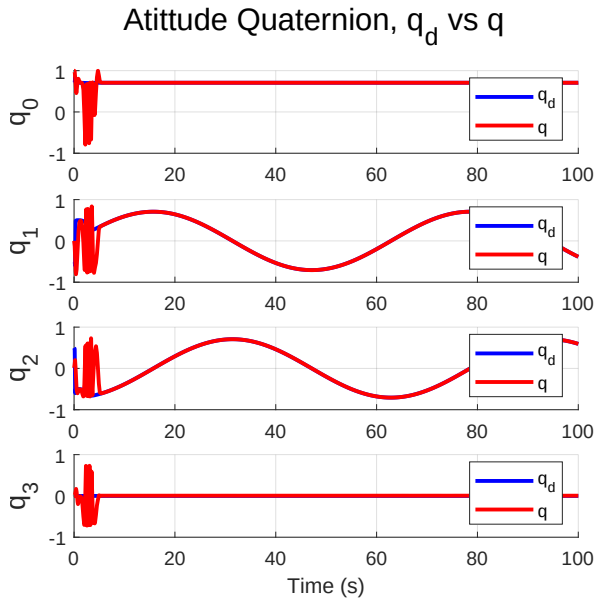

Figure 6: Desired quaternion ($\mathbf{q}_d$) vs Attitude quaternion ($\mathbf{q}$).

The $\tilde{\boldsymbol{\beta}}_v$ angle is shown in Fig. 7, where the SMC is able to compensate the effect of the disturbance and keep the error low.

The torques for the attitude stabilization of the vehicle are shown in the Fig. 8, these were limited to ± 1 N·m

4.2 SMC with ESO

For this case, the same initial conditions were applied, and using the following control gain: $l_1 = 250$, $l_2 = 400$, we get the trajectory shown in Fig. 9

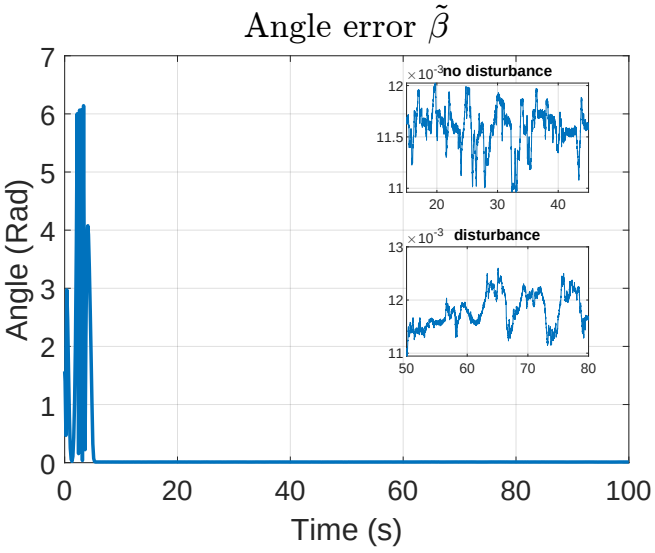

Figure 7: Error angle $\tilde{\beta}$.

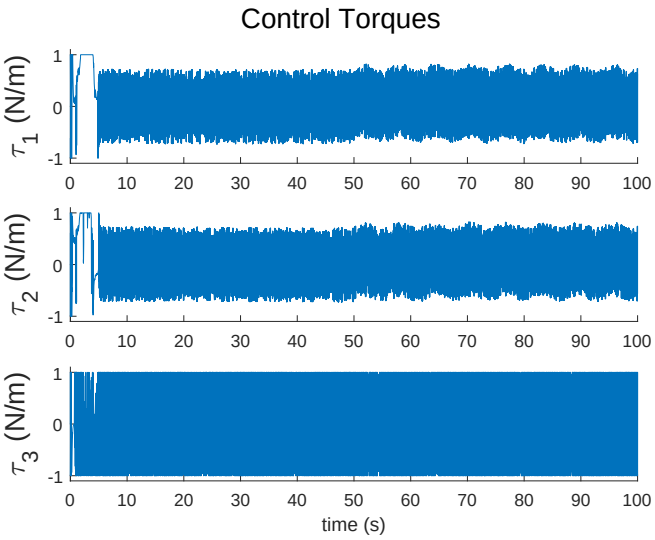

Figure 8: Control torques.

The trajectory errors are shown in Fig. 10.

The desired quaternion and the vehicle's attitude quaternion are shown in the Fig. 11.

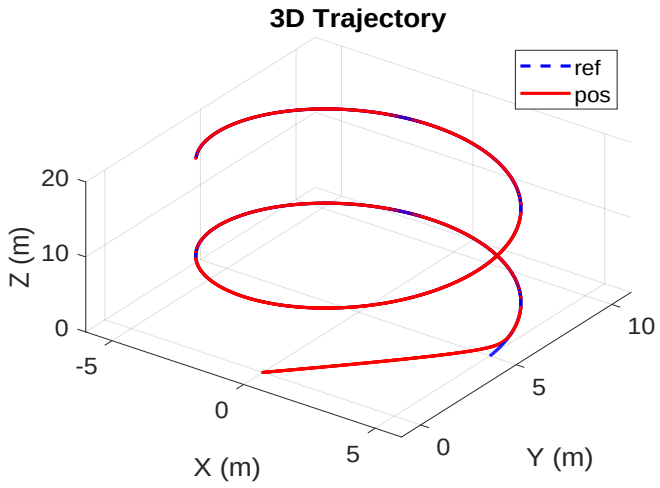

Figure 9: 3D spiral trajectory.

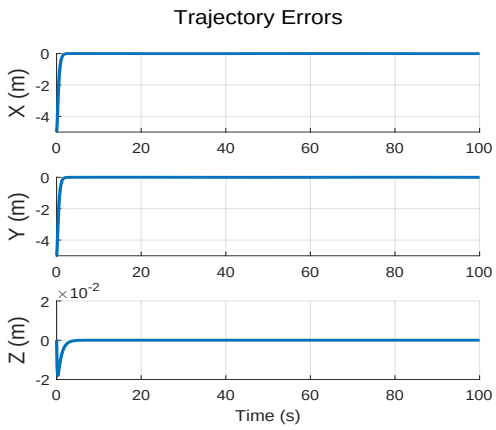

Figure 10: Errors in 3D trajectory.

The $\tilde{\beta}$ angle is shown in Fig. 12, as in the previous case, the error doesn't increase significantly when the disturbance in the input torques appears. The ESO keeps the error an order of magnitude lower than the previous case.

The torques for the attitude stabilization of the vehicle are shown in the Fig. 13, these also were limited to ± 1 N·m

Finally, the Integral Square Error (ISE) is shown in the Fig. 14, where an error of two orders of magnitude smaller error is observed when the ESO is added to the system

5 CONCLUSION

In this paper, we worked with the problem of the attitude stabilization and tracking of a quadrotor vehicle using a nonlinear sliding mode control approach. In addition, an ESO were proposed to estimate the inertia matrix uncertainties and unknown disturbances. Several simulations results are carried out in order to show the effectiveness of the proposed nonlinear control strategies and proving that an ESO is useful when there are uncertainties in the vehicle parameters.

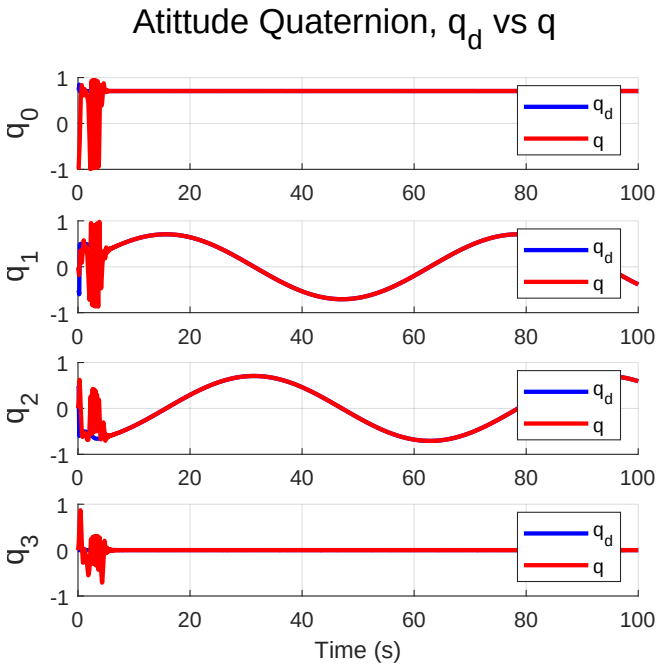

Figure 11: Desired quaternion ($\mathbf{q}_d$) vs Attitude quaternion ($\mathbf{q}$).

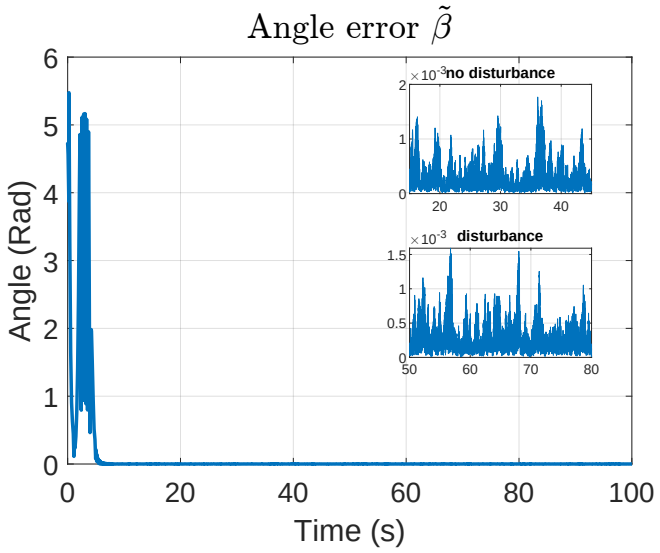

Figure 12: Error angle $\tilde{\beta}$.

ACKNOWLEDGMENTS

This work was made possible thanks to the CONACYT scholarship no. 546826 and the CONACYT Basic Science Project CB-2015-257985.

REFERENCES

[1] Gabe Hoffmann, Dev Gorur Rajnarayan, Steven L Waslander, David Dostal, Jung Soon Jang, and Claire J

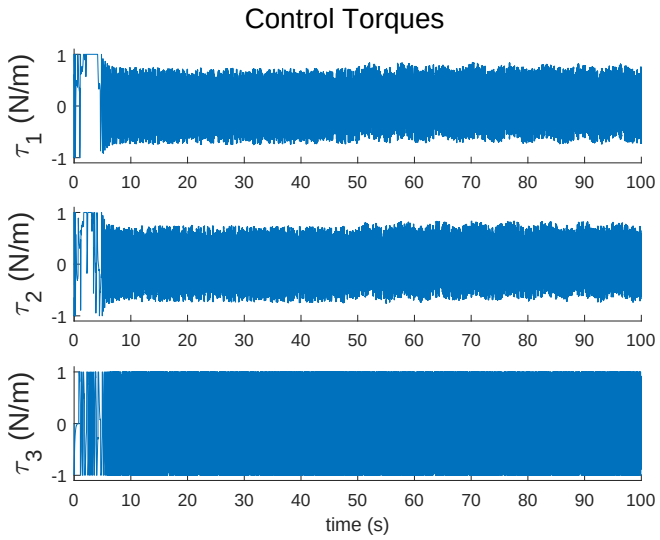

Figure 13: Control torques.

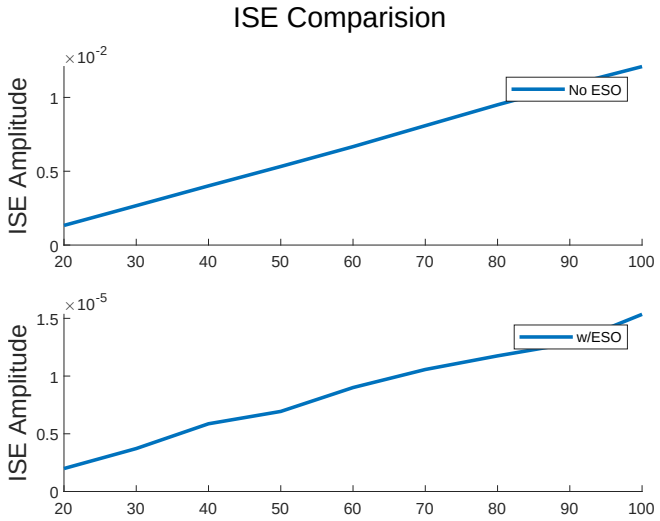

Figure 14: Control torques.

Tomlin. The stanford testbed of autonomous rotorcraft for multi agent control (starmac). In *The 23rd Digital Avionics Systems Conference (IEEE Cat. No. 04CH37576)*, volume 2, pages 12–E. IEEE, 2004.

[2] Minh-Duc Hua, Tarek Hamel, Pascal Morin, and Claude Samson. Introduction to feedback control of underactuated vtolvehicles: A review of basic control design ideas and principles. *IEEE Control Systems Magazine*, 33(1):61–75, 2013.

[3] Roberto Naldi, Michele Furci, Ricardo G. Sanfelice, and Lorenzo Marconi. Robust global trajectory tracking for underactuated vtol aerial vehicles using inner-outer loop control paradigms. *IEEE Transactions on Automatic Control*, 62(1):97–112, 2017.

[4] Ben Ammar Nour, Bouallegue Soufiene, and Haggege Joseph. Modeling and Sliding Mode Control of a Quadrotor Unmanned Aerial Vehicle. *3rd International Conference on Automation, Control, Engineering and Computer Science (ACECS)*, 3(1), 2016.

[5] G. Jithu and P. R. Jayasree. Quadrotor modelling and control. In *2016 International Conference on Electrical, Electronics, and Optimization Techniques (ICEEOT)*, pages 1167–1172, 2016.

[6] J. Fermi Guerrero-Castellanos, Nicolas Marchand, Ahmad Hably, Suzanne Lesecq, and Jérôme Delamare. Bounded attitude control of rigid bodies: Real-time experimentation to a quadrotor mini-helicopter. *Control Engineering Practice*, 19(8):790–797, 2011.

[7] H. Abaunza, P. Castillo, and R. Lozano. Quaternion Modeling and Control Approaches. *Handbook of Unmanned Aerial Vehicles*, pages 1–29, 2018.

[8] Cyrus Jahanchahi and Danilo P Mandic. A class of quaternion kalman filters. *IEEE Transactions on Neural Networks and Learning Systems*, 25(3):533–544, 2013.

[9] Erik B Dam, Martin Koch, and Martin Lillholm. *Quaternions, interpolation and animation*, volume 2. Citeseer, 1998.

[10] Gaopeng Bo, Liuyong Xin, Zhang Hui, and Wanglin Ling. Quadrotor helicopter attitude control using cascade pid. In *2016 Chinese Control and Decision Conference (CCDC)*, pages 5158–5163. IEEE, 2016.

[11] Elias Reyes-Valeria, Rogerio Enriquez-Caldera, Sergio Camacho-Lara, and Jose Guichard. Lqr control for a quadrotor using unit quaternions: Modeling and simulation. In *CONIELECOMP 2013, 23rd International Conference on Electronics, Communications and Computing*, pages 172–178. IEEE, 2013.

[12] Rafael Guardeño, Manuel J López, and Víctor M Sánchez. Mimo pid controller tuning method for quadrotor based on lqr/lqg theory. *Robotics*, 8(2):36, 2019.

[13] Samir Bouabdallah, Andre Noth, and Roland Siegwart. PID vs LQ control techniques applied to an indoor micro quadrotor. In *2004 IEEE/RSJ International Conference on Intelligent Robots and Systems (IROS)(IEEE Cat. No. 04CH37566)*, volume 3, pages 2451–2456. IEEE, 2004.

[14] Shahida Khatoon, Dhiraj Gupta, and LK Das. PID & LQR control for a quadrotor: Modeling and simulation. In *2014 international conference on advances in computing, communications and informatics (ICACCI)*, pages 796–802. IEEE, 2014.

[15] Xing Huo, Mingyi Huo, and Hamid Reza Karimi. Attitude stabilization control of a quadrotor uav by using backstepping approach. *Mathematical Problems in Engineering*, 2014, 2014.

[16] Paul De Monte and Boris Lohmann. Trajectory tracking control for a quadrotor helicopter based on backstepping using a decoupling quaternion parametrization. In *21st Mediterranean Conference on Control and Automation*, pages 507–512. IEEE, 2013.

[17] An Honglei, Li Jie, Wang Jian, Wang Jianwen, and Ma Hongxu. Backstepping-based inverse optimal attitude control of quadrotor. *International Journal of Advanced Robotic Systems*, 10(5):223, 2013.

[18] Jihad Ghandour, Samir Aberkane, and Jean-Christophe Ponsart. Feedback linearization approach for standard and fault tolerant control: Application to a quadrotor uav testbed. *Journal of Physics: Conference Series*, 570(8):082003, 2014.

[19] Young-Cheol Choi and Hyo-Sung Ahn. Nonlinear control of quadrotor for point tracking: Actual implementation and experimental tests. *IEEE/ASME transactions on mechatronics*, 20(3):1179–1192, 2014.

[20] Kostas Alexis, Christos Papachristos, Roland Siegwart, and Anthony Tzes. Robust model predictive flight control of unmanned rotorcrafts. *Journal of Intelligent & Robotic Systems*, 81(3-4):443–469, 2016.

[21] Gaetano Tartaglione, Egidio D'Amato, Marco Ariola, Pierluigi Salvo Rossi, and Tor Arne Johansen. Model predictive control for a multi-body slung-load system. *Robotics and Autonomous Systems*, 92:1–11, 2017.

[22] Ahmed T Hafez, Anthony J Marasco, Sidney N Givigi, Mohamad Iskandarani, Shahram Yousefi, and Camille Alain Rabbath. Solving multi-uav dynamic encirclement via model predictive control. *IEEE Transactions on control systems technology*, 23(6):2251–2265, 2015.

[23] Hongwei Mo and Ghulam Farid. Nonlinear and adaptive intelligent control techniques for quadrotor uav–a survey. *Asian Journal of Control*, 21(2):989–1008, 2019.

[24] Yuanqing Xia and Mengyin Fu. *Compound control methodology for flight vehicles*, volume 438. Springer, 2013.

[25] Zeghlache SAMIR. Sliding mode control strategy for a 6 dof quadrotor helicopter. *Journal of Electrical Engineering*, 10(3):7–7, 2010.

[26] Xingling Shao, Jun Liu, Huiliang Cao, Chong Shen, and Honglun Wang. Robust dynamic surface trajectory tracking control for a quadrotor uav via extended state observer. *International Journal of Robust and Nonlinear Control*, 28(7):2700–2719, 2018.

[27] John Dixon. *Suspension Analysis and Computational Geometry*. Wiley, 2009.

[28] Malcolm D Shuster. A survey of attitude representations. *Navigation*, 8(9):439–517, 1993.

[29] Rune Schlanbusch, Antonio Loria, and Per Johan Nicklasson. On the stability and stabilization of quaternion equilibria of rigid bodies. *Automatica*, 48(12):3135–3141, 2012.

[30] Anežka Chovancová, Tomáš Fico, Ľuboš Chovanec, and Peter Hubinsk. Mathematical modelling and parameter identification of quadrotor (a survey). *Procedia Engineering*, 96:172–181, 2014.

[31] Bin Xian, Chen Diao, Bo Zhao, and Yao Zhang. Nonlinear robust output feedback tracking control of a quadrotor uav using quaternion representation. *Nonlinear Dynamics*, 79(4):2735–2752, 2015.

[32] Yong Zhang, Zengqiang Chen, and Mingwei Sun. Trajectory tracking control for a quadrotor unmanned aerial vehicle based on dynamic surface active disturbance rejection control. *Transactions of the Institute of Measurement and Control*, 42(12):2198–2205, 2020.